A NEW STRAIGHT LINE RECONSTRUCTION METHODOLOGY FROM MULTI-SPECTRAL STEREO AERIAL IMAGES

A. O. Ok [a, *], J. D. Wegner [b], C. Heipke [b], F. Rottensteiner [b], U. Soergel [b], V. Toprak [a]

[a] Dept. of Geodetic and Geographic Information Tech., Middle East Technical University, 06531 Ankara, Turkey
- (oozgun, toprak)@metu.edu.tr
[b] Institute of Photogrammetry and Geoinformation, University of Hannover, 30167 Hannover, Germany
- (wegner, heipke, rottensteiner, soergel)@ipi.uni-hannover.de

Commission III - WG III/4

KEY WORDS: pair-wise line matching, line reconstruction, straight line extraction, stereo aerial images

ABSTRACT:

In this study, a new methodology for the reconstruction of line features from multispectral stereo aerial images is presented. We take full advantage of the existing multispectral information in aerial images all over the steps of pre-processing and edge detection. To accurately describe the straight line segments, a principal component analysis technique is adapted. The line to line correspondences between the stereo images are established using a new pair-wise stereo matching approach. The approach involves new constraints, and the redundancy inherent in pair relations gives us a possibility to reduce the number of false matches in a probabilistic manner. The methodology is tested over three different urban test sites and provided good results for line matching and reconstruction.

1. INTRODUCTION

Reliable extraction of corresponding lines in overlapping images can be used for different purposes such as 3D object extraction, improving the automated triangulation, image registration, motion analysis etc. Therefore, line matching is a challenging task, and still a vivid field of research. Up to now, a significant number of research papers have been published in this field; here, we only review the methods developed to extract 3D line features from aerial images. A useful classification of existing line matching approaches was proposed by Schmid and Zisserman (1997). They divided the line matching algorithms into two types, (i) those that match individual line segments, and (ii) those that match groups of line segments. In any case, the search space for matches has to be pruned in some way in order to limit complexity. For most of the studies, basic geometric parameters of line segments such as orientation, length, mid-point, etc. are involved to filter the set of correspondence hypotheses; however, probably the most preferred constraint is the quadrilateral constraint generated using the epipolar geometry (Collins et. al., 1998; Noronha and Nevatia, 2001; Kim and Nevatia, 2004; Suveg and Vosselman, 2004). Some studies also integrated the radiometric information around the line segments along with the geometrical primitives (Henricsson, 1998; Scholze et. al., 2000; Zhang and Baltsavias, 2000). Additional constraints such as uniqueness and ordering (Suveg and Vosselman, 2004), figural continuity (Zhang, 2005) can also be included; however, even for a simple stereo line matching problem, these constraints are not sufficient to solve the image to image multi-correspondence problem. Thus, additional effort has been spent on different algorithms to select the best line correspondences. For example, dynamic programming (Yip and Ho; 1996), weighted criterion functions (Henricsson, 1998), modal analyses (Park et. al., 2000), and probability relaxation (Zhang and Baltsavias, 2000; Zhang, 2005) are among those approaches. On the other hand, additional view(s) can also be incorporated in the line matching stage; some examples can be found in Schmid and Zisserman (1997), Collins et. al. (1998), Noronha and Nevatia (2001), and Kim and Nevatia (2004).

Pair-wise stereo line matching is also introduced in several studies; for example, Park et. al. (2000) proposed a matching approach which takes into account only geometric relations between the lines. However, they assumed that the lengths and angles between the lines in a pair are almost exact copies of each other. Zhang and Baltsavias (2000) proposed a pairwise edge matching approach using relaxation labelling for 3D road reconstruction. Due to the

nature of the relaxation algorithms, the smoothing effects and the issue of convergence with a large execution time could be the main concerns. Noronha and Nevatia, (2001), and Kim and Nevatia (2004) proposed a pair-wise approach based on the epipolar geometry. However, they utilize multiple images to reduce the pair-wise ambiguities and due to constraint of orthogonality, their approach is restricted for the line pairs detected over rectilinear flat objects.

So far, in a stereo environment, the ambiguity problem of line matching is an issue that remain unsolved. The major problem arises from the lack of measure(s) and/or constraint(s) for line features that are invariant under different viewing conditions. Up to now, the general attempt to reduce the ambiguity problem is to strengthen the geometrical constraint by integrating one or more additional views (Schmid and Zisserman, 1997; Collins et. al., 1998; Noronha and Nevatia, 2001; Kim and Nevatia, 2004; Zhang, 2005). Several others utilized external DSMs (Jung and Paparoditis, 2003; Taillandier and Deriche, 2004) or supplementary matched point features (Zhang, 2005) for both reducing the search space and filtering out the matching ambiguities. Nevertheless, the final matching performance of those algorithms is highly dependent and determined by the efficiency and the quality of those auxiliary datasets. On the other hand, the probabilistic relaxation based methods (Zhang and Baltsavias, 2000; Zhang, 2005) utilize the predefined local neighbourhood information which mostly suffer from the piecewise smoothness constraints involved. Inevitably, smoothing based on the local neighbourhood violates the standpoint of height discontinuity (except artificial edges such as shadows etc.) of the edges and the subsequent line matching.

One important different aspect from the review of the literature is that while aerial images have been rich of multispectral information, this fact was completely discarded or not efficiently used during the low level processing such as filtering, edge detection etc. However multispectral aerial images provide opportunities to extract line features that cannot be detected in the grayscale images (Scholze et. al., 2000, Koschan and Abidi, 2005) due to several reasons, such as low contrast, accidental object alignments etc.

2. METHODOLOGY

In this study, we introduce a new methodology for the 3D reconstruction of line features from multispectral stereo aerial images. In order to maximize the line detection completeness, we take full advantage of the existing multispectral information in aerial images throughout the steps of pre-processing and edge

---

* Corresponding author.

detection. To accurately describe the straight edge segments, a principal component analysis technique is adapted. To establish the line to line correspondences between the stereo images, a new pair-wise stereo matching approach is developed. The approach involves new constraints and a final probabilistic elimination to reduce the number of false matches.

2.1 Pre-Processing

2.1.1 Multi-level Non-Linear Color Diffusion Filter: The aim of the non-linear diffusion filtering is to eliminate the noise inherent in the images without blurring the step discontinuities. A good review related to diffusion filters can be found in (Weickert, 1997). Since we deal with multispectral images, it is important to perform the filtering procedure considering those discontinuities in different bands. In order to achieve this, we adapted a gradient computed through tensor mathematics (see section 2.2.1) to improve the performance of the original non-linear filter. In addition, we utilized a three level processing chain (decreasing the sigma parameter while increasing the lambda parameter) to diminish the noise around the step discontinuities.

2.1.2 Color Boosting: The goal of color boosting is to improve the apparent color difference between adjacent objects in a scene. For the aerial images (especially for analog cameras), the contrasts in the RGB values caused by the color variations are generally not high enough to exploit this distinction. Therefore, the idea is to amplify the color variations between the objects (for example, a building roof and its background) before the edge detection to find the edges that cannot be detected due to low color variation. We utilized the boosting technique developed by Weijer et. al. (2006a). First, the RGB color space is transformed to the decorrelated Opponent Color Space (o1, o2, and o3). Next, to improve the color contrast in the images, color directions of the opponent space (o1 and o2) are selected and multiplied with a factor of k (k>1). Finally, the modified opponent color space is back-transformed to RGB color space.

2.2 Line Extraction

2.2.1 Color Edge Detection: In this study, to maximize the performance of the edge detection, we utilize the algorithm developed in Weijer et. al. (2006b). They proposed a color Canny edge detection algorithm to locate the edges accurately in multispectral images. The algorithm mainly consists of the calculation of the spatial derivatives of the different image channels, and the computed derivatives are combined using tensor mathematics. In this way, differential structures of the bands in multispectral images are mutually supported, so that edge detection of better completeness is accomplished compared to the single band detectors. Two minor adaptations enhance the results of the algorithm: (i) the output of the final gradient map is scaled between zero-and-one before further processing, which significantly reduces the remaining noisy edges, and (ii) a two level hysteresis thresholding is designed to have a better control on the final edge contours (Fig. 1c, 1d).

2.2.2 The Extraction of the Straight Line Segments: We offer a two stage solution to the straight line extraction problem, (i) the extraction of straight edge segments, and (ii) robustly fitting line segments to the extracted straight edge segments.

We use the principal component analysis technique developed to extract the straight edge segments. The details of the method can be found in Lee et. al. (2006). Although the method has proven to be more efficient in several ways than Hough Transform (Lee et. al., 2006), we experienced several problems during the extraction of the straight edge segments. First, the input binary edge images are assumed to be segments that are only a single pixel wide. However, this is not the case for the output of the binary images generated by
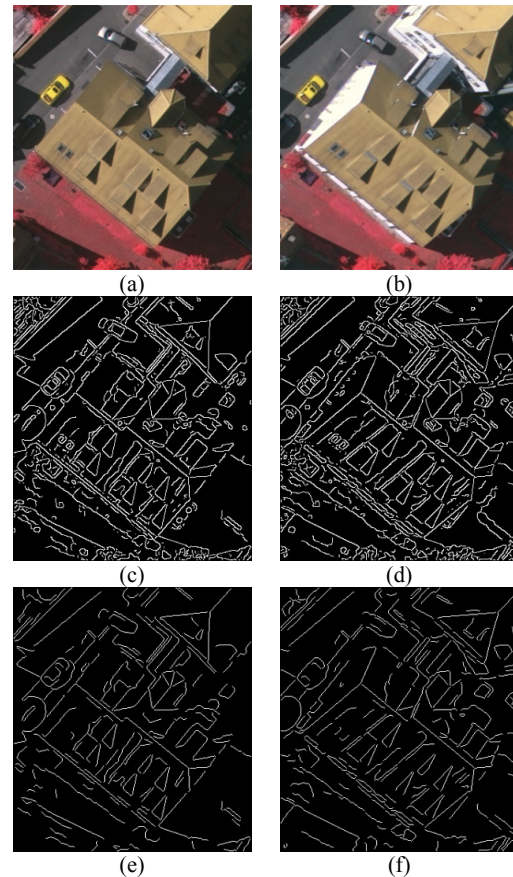

Fig. 1 (a, b) Test images from Vaihingen, Germany, (c, d) the results of the color Canny algorithm, (e, f) straight edge segments.

the color canny edge detection. Although non-maximum suppression is applied after the detection stage, this does not always guarantee one pixel wide edges for color images, since separate spatial derivatives of the image bands are combined during edge detection. In this study, we utilized the image skeleton technique to remove the redundant boundary pixels of the binary edges. The technique ensures that the binary objects shrink to a minimally connected structure without breaking apart. A different critical shortcoming we observed is that, if two same label (for example two column-directional) binary edge segments are connected with a junction of a narrow angle, the algorithm is no more capable to determine the correct straightness value. Unfortunately, this type of line to line combinations is not rare in aerial images. To solve the problem, we identified all potential line to line (or multi-line) endings and crossings within each segment. Thereafter, the problematic crossings of the edge segments are removed.

We refer to a line segment as a single straight object that is composed of only two endpoints $(x_1, y_1; x_2, y_2)$. To accurately describe the line segments, in this study, the well-known Ransac algorithm is utilized (Fischer and Bolles, 1981; Zuliani et. al., 2005). In some cases, a single straight edge segment may be represented by more than a single straight line. For those cases, a recursive strategy is applied to describe each line segment from the straight edge segments. Fig. 3a and 3b illustrates the line segments extracted for the images given in Fig. 1a and 1b.

2.3 Pair-wise Stereo Line Matching

Once the straight lines are extracted, a matching strategy is required to find the line correspondences between the reference and search images. We propose a new pair-wise stereo line matching strategy that consists of two fundamental stages: (i) selection of line pairs on the reference image, (ii) identifying the candidate pair models on the search image.

During the implementation, for the realization of the image-to-image relations (estimation of the epipolar lines, stereo intersection etc.), we utilized well-known photogrammetric techniques. For this study, we assumed that the processed stereo images are not significantly different (within ±5°) in terms of their kappa (κ) angles. Thus, we do not apply any a priori rotation to the line segments for the calculation of their angle values in image space.

2.3.1 Selection of Line Pairs on the Reference Image: In urban areas the number of extracted lines is quite large even for a small part of an aerial image. Our aim is to search for pairs of lines that have a connection in terms of their height values, and to discard those pair-wise relations that do not show any reasonable similarity. Since the height values of lines are not known at this stage, we assess three criteria, (i) proximity, (ii) angle of intersection in image space, (iii) similarity of the radiometric values in the flanking regions, during the selection of the line pairs.

The first measure, proximity (T_{prox}), defines the minimum 2D Euclidean distance (d_{ij}) between two lines (l_i and l_j) (Fig. 2a). It can be defined as a joint minimum of two Euclidean distances; the minimum distance between the endpoints of the line segments in a pair, and the minimum of the orthogonal distances computed from one of the lines of any point on the other line segment. For example in Fig. 2a, the shortest 2D distance between the line segments l_1 and l_4 is the d_{14} distance.

The second measure is the angle enclosed by line segments l_i and l_j (Fig. 2b). In this study, we only allow formations of line pairs that have a finite intersection point (not parallel) and an angle of intersection value larger than a specific threshold ($\geq T_{ang}$). In Fig. 2b, the line segments, l_1 and l_3 have approximately similar orientation, therefore, the pair grouping of l_1 and l_3 is not allowed.

The third measure, similarity of flanking regions, is another metric to evaluate the selection of line pairs. Apparently, if the lines in a pair do not show any similarities within their flanking regions, those lines can be assumed to be part of different objects. In this study, for each line, left and right flanking regions are generated, and the robust radiometric mean values of the pixels within the flanking regions are estimated using the minimum covariance determinant (Meucci, 2005). The similarities can be computed in several ways and may involve different color spaces (Henricsson, 1998; Zhang and Baltsavias, 2000); however; we utilized the multispectral bands directly for the computation of the similarities by taking the absolute differences of the norms of the mean values. One other important gain that we achieve at the end of this process is that, the comparison of the flanking regions gives us ability to learn which side(s) of a pair represents the most similarity. This information is also held in reserve to be used in the next stage, identifying candidate pair models on the search image.

2.3.2 Identifying Candidate Pair Models on the Search Image: Once all line pairs are selected from the reference image, their corresponding matches on the other image is also searched using a pair-wise approach. To fulfil this objective, for each reference pair, all candidate pair models must be collected from the other image. With the knowledge of the exterior and interior orientation along with the user-specified minimum and maximum height values (or the approximated height information derived from a DSM data), for a single line, an epipolar quadrilateral region constraint can be employed to reduce the search space (Schmid and Zisserman, 1997; Zhang and Baltsavias, 2000). However, in a pair-wise strategy, there are two lines in a pair; thus, we collect all candidates for a pair of lines using two different quadrilateral regions. For example, in Fig. 3b, two quadrilateral regions (defined by certain minimum and maximum height) are illustrated for the line pairs, l_1 and l_2 (Fig. 3a). However, even for a single line, the number of candidates in each quadrilateral region could be excessive. Here, we propose a constraint to construct the candidate pair model sets from the individual candidates. As a result, for each
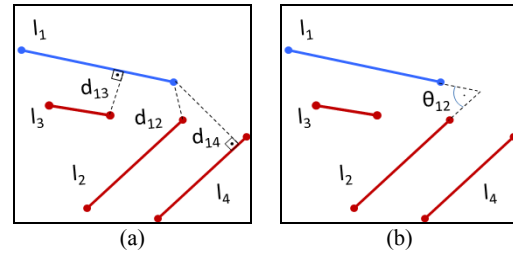

Fig. 2 Lines on the reference image, (a) the proximity measure, (b) the angle of intersection.

line, we can reduce the number of candidates considerably. We first compute the intersection point of the reference pair (Fig. 3c). Since, we restricted the formation of the reference pairs in the previous stage with a specific angle ($\geq T_{ang}$, see section 2.3.1); there is always an intersection point between the lines that form a reference pair. After that, we estimate the epipolar line segment (with the same minimum and maximum heights) of the intersection point on the search image (Fig. 3d). Next, for all candidate pair models, we computed their individual intersection points and tested the proximity of the points to the epipolar line segment by computing their orthogonal distances. If the distance value is computed to be less than a threshold (T_{epi}), the candidate pair is justified, otherwise deleted. For the threshold T_{epi}, rigorous experimental evaluations are performed, and we found that almost all the correct pair intersections are within the range of 5 pixels distance to the epipolar line. Very similar results for the features of junctions are already verified by (Kim and Nevatia, 2004), thus we fixed the parameter T_{epi} to 5 pixels. The intersection points of candidate pair models that are computed to be less than T_{epi} for the line pair l_1 and l_2 are shown in Fig. 3d.

Although the epipolar line of intersection constraint is very successful if the lines in a pair actually intersect on the Earth surface (or intersect hypothetically), it does not hold for the pairs that are formed by the lines that do not intersect. Thus, the correct pair model (if it exists) on the other image might be missed. However, those kinds of pair formations are minimized through the selection step by imposing the flanking regions constraint (see section 2.3.1). One different aspect of this constraint is that, it also automatically eliminates the pairs in which two lines in one view
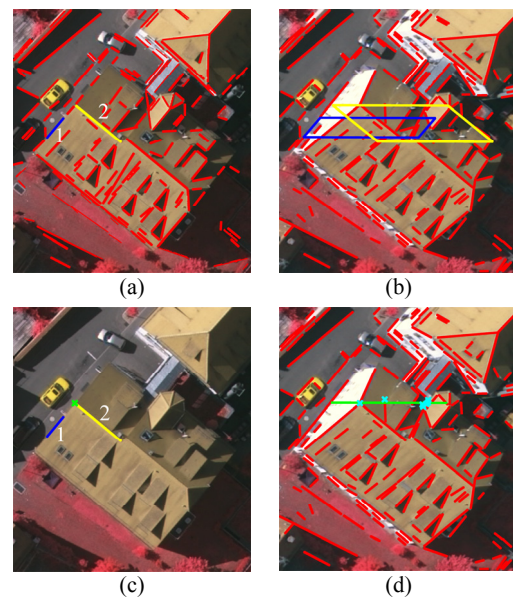

Fig. 3 (a) reference line pairs, (b) the quadrilateral regions, (c) the intersection point of l_1 and l_2, (d) the epipolar line of intersection and the intersections of candidate pair models that are computed to be less than T_{epi}.

27

correspond to a single line in the other view (lack of a unique intersection point). To solve these cases, we use the repetitive nature of the pair formation considering the fact that a single line is allowed to have a part in different pair models. Thus, a single line has possibility to be matched with its correct correspondences in different pair models.

In order to describe the geometrical relations between the line segments in a pair, we employ three different measures (Park et. al., 2000). First measure is the angle which two line segments l_1 and l_2 form, the second measure is the directional angle from the midpoint of l_1 to that of l_2, which is the angle measured from the first line to the second line, and the third measure is the ratio of the sum of line segments to the average distance between the endpoints of the line segments (Park et. al., 2000) (Fig. 4a). However, in most of the cases, the last two geometrical relations are inappropriate for aerial images, since the line segments found in different views may have different lengths and midpoints due to several reasons such as occlusion, image noise etc. In addition, the perspective distortion combined with relief of terrain and/or of individual objects also plays an important role at this point and in cumulative, the measures become inconsistent from one view to another. Assume that the lines c_1 and c_2 in Fig. 4b are forming one of the candidate pair models of the lines l_1 and l_2 in Fig. 4a. If we compare the lengths of the lines in each pair, only the length of the line c_2 is significantly different; however, even in this case, two geometrical measures computed are different from each other. We propose a normalization scheme to deal with the problems of the geometrical reliability of the line segments extracted from different views. It relies on the epipolar geometry and the idea of finding the overlaps of lines in different views. We utilize the endpoints of each line and estimate the epipolar lines on the other view. Thus, we perform a point to point correspondence (Schmid and Zisserman, 1997) on each line to provide a final single overlapping line for each line in a pair (Fig. 4c- and 4d-left). We apply this normalization scheme for each reference pair and its candidate pair model before the computation of the second and third geometrical measures. Thus, the measures become reliable (Fig. 4c- and 4d-right) when compared to their non-normalized counterparts.

As additional constraints, we propose two different flanking region constraints for a reference pair and their candidate pairs; (i) the intra-pair similarity, and the inter-pair similarity. The former measure takes into account the similarity of the side(s) of the reference pair model previously found (see section 2.3.1) and searches whether a similar relationship of the flanking information of the same sides for the candidate pair models exist or not. If it exists, the latter measure considers the similarity of flanking regions of the line segments individually. To allow such constraint, the illumination of the images is assumed to be similar (the case in

a single strip acquisition) and the reflections are assumed to comply with the lambertian theory.

In this study, we propose two new additional constraints to the stereo pair-wise line matching scheme; a correlation constraint forced on a hypothesized 3D triangular plane and a spatiogram constraint that deals with the regional similarity dominated by the reference line pair and the candidate pair models.

The correlation constraint performs on a 3D plane fitted to the line pairs and their intersection point based on the assumptions that (i) they are the correct match, and (ii) they belong to a single plane. A correlation measure bounded for all the area marked by the 3D lines and the intersection point is not appropriate, since there may be different planes on a building roof (chimneys, dormers etc). Thus, we apply the correlation measure to the immediate vicinity of the point of intersection and the corresponding plane, which can also be defined as a 3D triangular plane (Fig. 5a and 5b). We fixed the side lengths of the triangle which are exactly on the same direction of the lines by a single distance parameter d = 2 m. Fig. 5a and 5b illustrate the extents of the back projected plane that is estimated through the line pairs given in the figure. However, there may be several cases that may violate the plane formation and the correlation value computed; (i) the intersection point of the lines that are exactly on the same plane may occur on a different plane(s) than their own plane (Fig. 5c – pair$_{AB}$) (ii), the lines that really intersect on the Earth surface may not form a plane (Fig. 5c – pair$_{CD}$), and (iii) the planes formed by the line pairs may be hidden or occluded in one view (Fig. 5d – pair$_{EF}$). It is straightforward to track the last violation; we compute the angle of the plane with its projected plane (to a flat terrain), and only apply the correlation measure if the computed plane angle is narrower than a specific angle threshold ($\leq 75°$). However, the other two violations cannot be handled in a similar manner, since the hypothesized 3D planes are not correct. Thus, based on our rigorous experiments, we decided to fix the threshold of the measure of correlation to a very relaxed constant ($T_{cor} \geq 0.2$), and utilized the constraint to eliminate the candidate pair models that show no or negative correlation.

Finally, the regional similarities dominated by the reference line pairs and the candidate pair models are evaluated. We select the 2D regions that are consistently described by the line pairs. However, it is simply impossible to compare the regions directly, since the perspective distortion and the features belong to many different planes on the roofs may simply alter the positions of the pixels to some extent. On the other hand, it is not logical to compare the regions with a simple histogram measure, since many parts of the images may contain similar radiometric information; very different regions generally produce similar histograms. Therefore, we utilize the spatiogram measure to evaluate the regional similarity between the regions. A very important aspect of the spatiogram measure is
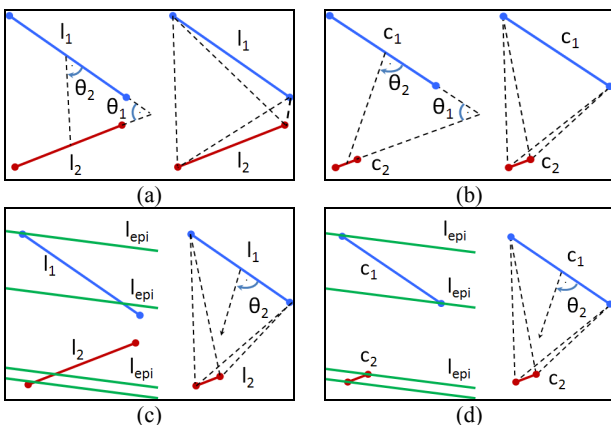

Fig. 4 (a) The geometrical measures utilized, (b) a candidate pair model and its geometrical measures, (c) and (d) normalization with epipolar lines and the normalized measures.
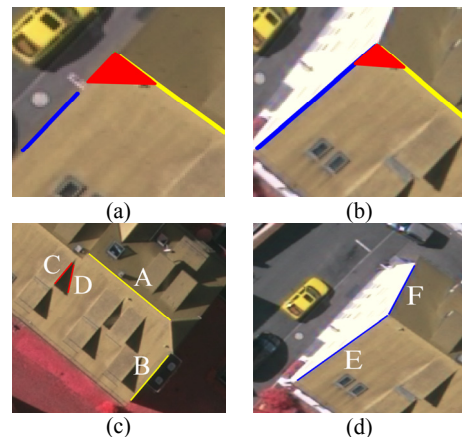

Fig. 5 (a, b) The back projected plane estimated from the line pairs, (c, d) several cases that may violate the plane constraint.

that it has a unique capability to combine the distribution of the radiometric information along with the spatial information. Thus, the positional differences occur between the line pairs are handled (somewhat alleviated) while providing the histogram information. The details of the algorithm are explained in (Ó Conaire et. al., 2007), for our case, we fixed the number of bins to 8 for each band and applied a spatiogram similarity threshold of $T_{spatiogram} \geq 0.75$ (between 0 and 1) for regional similarity comparison.

The final pair matches are assigned after a weighted pair-wise matching similarity score which is computed over a total of eight measures; an epipolar, three geometric, two photometric, a correlation and a spatiogram measure. All the measures are normalized from 0 to 1 prior to the calculation, and the total similarity result is computed as the average of all similarities. However, the pair-wise matching does not always guarantee one to one matches for each line. Once all the pair-wise matches are collected, a probabilistic reasoning is applied to solve the matching ambiguity problem. Since a single line is allowed to have a part in different pair models, after the pair-wise matching stage, we have generally sufficient number of matching redundancy for lines. Thus, we have possibility to eliminate particular false line matches using this redundancy. In this study, we selected the best line correspondences with a single probability threshold ($p \geq 0.6$). In general, the threshold is exceeded for most of the ambiguities and provided very good results. If the probability value computed is found to between 0.5 and 0.6, in this study, we keep all the line matches. For an immediate future work, our aim is to design a better decision scheme by applying a higher level probabilistic post-processing.

3. RESULTS AND DISCUSSION

We processed three urban test sites from Germany to assess the performance of our methodology. The first image pair was acquired over a densely built up area of the city of Vaihingen (Fig. 6 – 1st column) by the DMC digital camera with 70% forward overlap (Cramer and Haala, 2009). The focal length of the camera was 120 mm and the flying height was approximately 800 m above the ground level which corresponds to a final ground sampling distance (GSD) of approximately 8 cm. The second image pair (© Geoinformation Hannover) belongs to the Schneiderberg region of Hannover (Fig. 6 – 2nd column). The images were taken with RMK TOP30 analog camera with standard 60% forward overlap. The calibrated focal length of the camera was 305.560 mm with a flying height of approximately 1600 m. The images were scanned at 14-µm resolution and this corresponds to a final GSD of 7-cm. The third image pair (© Geobasisdaten: Land NRW, Bonn, 2111/2009) was acquired from the city of Dorsten (Fig. 6 – 3rd column) where the stereo pairs are acquired with DMC camera with 55% percent forward overlap. The flying height was around 2000 m above the ground level; thus, the GSD of the images was around 20 cm.

For all test sites, the number of correct and false line matches was assessed manually and the number of correct matches is computed to be higher than 92% (Table 1). Similarly, the number of false matches for all sites is comparable; however, the highest number of false matches (8%) is computed for the Hannover image pair. In fact, this is an expected result, since the images of the Hannover dataset were taken by an analog camera and scanned afterwards. Thus, the quality of the images and the noise level involved has probably affected the quality of the extracted lines. For each test

Test Site	# of lines		Matches		
	Left	Right	Total	Correct	False
Vaihingen	1726	1875	963	909 (94%)	54 (6%)
Hannover	2339	2369	1038	954 (92%)	84 (8%)
Dorsten	2724	2764	1598	1516 (95%)	82 (5%)

Table 1. The matching results of the proposed methodology.

Lines having	Number of		RMS Distance	
	Lines	Planes	cm	pixels
1-neighboring plane	21	21	12.7	1.59
2-neighboring planes	38	76	13.9	1.74
no plane	1	-	-	-
Total	60	97	13.6	1.70

Table 2. RMS distances between the reconstructed lines and neighbouring planes

site, if we compare the total number of matches with respect to the number of lines found in each image, the highest percentage of matching (58%) was achieved for the Dorsten image pair. This can be explained with the characteristics of the buildings in the test site, since most the buildings have less detail and complexity with respect to the other test sites. In addition, the spatial resolution of the image pair used is relatively coarse (20 cm), thus, most of the lines extracted belong to the main body of the buildings which is suitable to be matched using a pair-wise approach.

For the Vaihingen data set, the accuracy of the reconstructed lines could be evaluated by comparing them to LIDAR data. The LIDAR data of the test site were captured with a Leica ALS50 system with an accuracy of 3.4 cm (Haala, 2009). In order to compare the reconstructed lines, we randomly selected 60 reconstructed 3D lines and automatically extracted 3D planes from the point cloud in the vicinity of each line. Depending on the type of the line, this plane reconstruction process resulted in one plane if the line corresponded to a step edge and in two planes if the line corresponded to the intersection of two planes. In one case no such planes could be found. For each of the 59 lines, we determined the line's average orthogonal distance from its neighbouring planes and used these distances to compute the RMS average distance between the reconstructed lines and the LIDAR planes. The RMS distance was determined separately for lines corresponding to one plane and those corresponding to two; furthermore, a total RMS distance was also determined (Table 2). The total RMS distance, based on 59 lines and a total of 97 planes, was 13.6 cm. This corresponds to 1.7 pixels in the original images (GSD 8 cm). Several different error sources (inaccuracies during line extraction, epipolar alignment problem, the accuracy of the reference data itself etc.) may be involved in this result. As we used a simple perspective model without any additional parameters for the image orientations, we believe that a considerable portion of the error budget may come from the un-modelled systematic errors.

4. CONCLUSIONS AND FUTURE WORK

A new approach for the reconstruction of 3-D line segments from multispectral stereo aerial images was proposed. The following aspects outline the contributions of our approach: (i) the methodology take full advantage of the existing multispectral information in aerial images all over the steps especially during the pre-processing and edge detection. Thus, even building boundaries that show only a very slight color difference could be detected. (ii) With the improvements performed to the straight edge detector, the straight line extraction algorithm works quite robust, even for the areas where an enormous number of edges were found. This offers an opportunity to detect and reconstruct lines that belong to buildings and their certain details. (iii) To establish the line correspondences between the stereo image pairs, a new pair-wise stereo matching approach is presented. The approach involves new constraints, and the redundancy inherent in pair relations gives us possibility to reduce the number of false matches with a probabilistic manner.

The final results of the methodology are encouraging. Our approach shows good results for the stereo line matching and 3D line reconstruction for the buildings located in dense and complex environments. For an immediate future work, our aim is to design a better decision scheme by applying a higher level probabilistic
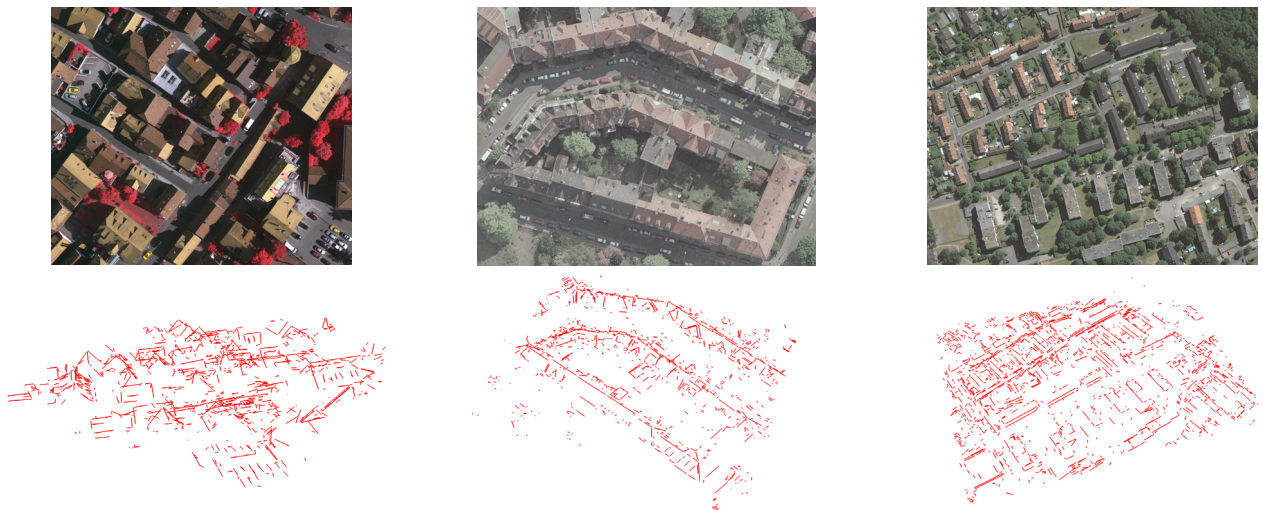
Fig. 6 Test sites (first row - from left to right - Vaihingen, Hannover, and Dorsten), and the results of the reconstruction (second row)

post-processing. Besides, to mitigate the occlusion problem of the stereo environment, additional views can be integrated and processed in the same manner. Inspired by (Kim and Nevatia, 2004), the main challenge of future work will be how to integrate and combine the lines that are reconstructed from different stereo image pairs.

ACKNOWLEDGEMENTS

REFERENCES

Cramer, M., Haala, N., 2009. DGPF Project: Evaluation of digital photogrammetric aerial based imaging systems – overview and results from the pilot centre. In: *International Archives of the Photogrammetry, Remote Sensing and Spatial Information Sciences* XXXVIII (1-4-7/W5), CD-ROM.

Collins, R. T., Jaynes, C. O., Cheng, Y. Q., Wang, X., Stolle, F., Riseman, E. M., and Hanson, A. R., 1998. The Ascender System: Automated Site Modeling from Multiple Aerial Images. *Computer Vision and Image Understanding*, 72(2), pp. 143-162.

Fischer, M. and Bolles, R., 1981. Random Sample Consensus: A Paradigm To Model Fitting With Applications To Image Analysis And Automated Cartography, *CACM* 24 (6), pp. 381–395.

Haala, N., 2009. Come Back of Digital Image Matching. *Photogrammetric Week*, Stuttgart, Germany.

Henricsson, O., 1998. The Role of Color Attributes and Similarity Grouping in 3-D Building Reconstruction. *Computer Vision and ImageUnderstanding*, 72(2), pp. 163-184.

Jung, F., Paparoditis N., 2003. Extracting 3D free-form surface boundaries of man-made objects from multiple calibrated images: a robust, accurate and high resolving power edgel matching and chaining approach. In: *IAPRS,* 34 (Part 3/W8).

Kim, Z., and Nevatia, R., 2004. Automatic Description of Complex Buildings from Multiple Images, *Computer Vision and Image Understanding*, 96(1), pp. 60-95.

Koschan, A., and Abidi, M., 2005. Detection and Classification of Edges in Color Images," *IEEE Signal Processing Magazine*, Special Issue on Color Image Processing, 22(1), pp. 64-73.

Lee, Y., Koo, H., Jeong, C., 2006. A Straight Line Detection Using Principal Component Analysis, *Pattern Recognition Letters*, 27, 1744-1754.

Meucci, A., 2005. *Risk and Asset Allocation*, Springer, pp. 209 – 229.

Noronha, S., and Nevatia, R., 2001. Detection and Modeling of Buildings from Multiple Aerial Images, *IEEE Transactions on Pattern Analysis and Machine Intelligence*, 23(5), pp. 501-518.

Ó Conaire, C., and O'Connor, N. E., and Smeaton, A. F., 2007. An improved spatiogram similarity measure for robust object localisation. In: *ICASSP*, Hawaii.

Park, S., Lee, K., and Lee, S., 2000. A Line Feature Matching Technique Based on an Eigenvector Approach, *Computer Vision and Image Understanding*, 77, pp. 263-283.

Schmid, C. and Zisserman, A., 1997. Automatic Line Matching Across Views. In: *Proceedings of CVPR*, pp. 666–671.

Scholze, S., Moons, T., Ade, F., Van Gool, L., 2000. Exploiting Color for Edge Extraction and Line Segment Stereo Matching. In: *IAPRS*, 815–822.

Suveg, I., and Vosselman, G., 2004. Reconstruction of 3D Building Models from Aerial Images and Maps, *ISPRS Journal of Photogrammetry and Remote Sensing*, 58, pp. 202-224.

Weickert, J., 1997. A Review of Nonlinear Diffusion Filtering, Scale Space Theory in Computer Vision, Lecture Notes in Computer Science, vol. 1252, Springer, pp. 3-28.

Weijer, J., Gevers, T., and Bagdanov, A.D., 2006a. Boosting Color Saliency in Image Feature Detection, *IEEE Transactions on Pattern Analysis and* Machine Intelligence, 28(1) pp. 150-156.

Weijer, J., Gevers, T., and Smeulders, A.W.M., 2006b. Robust Photometric Invariant Features from the Color Tensor, *IEEE Transactions on Image Processing*, 15(1) pp. 118-127.

Yip, R. K. K., and Ho, W. P., 1996. Multi-level Based Stereo Line Matching with Structural Information Using Dynamic Programming, In: *International Conference on Image Processing*, 2, pp. 341-344.

Taillandier F., Deriche, R., 2004. Automatic Buildings Reconstruction from Aerial Images: a Generic Bayesian Framework. In: *IAPRS*, 35 (Part 3A).

Zhang, C., Baltsavias, E. P., 2000. Edge matching and 3D road reconstruction using knowledge-based methods, Schriftenreihe der Fachrichtung Geodaesie, Darmstadt, Germany, 10, pp. 251-265.

Zhang, L., 2005. Automatic Digital Surface Model (DSM) Generation from Linear Array Images, PhD Thesis, Swiss Institute of Technology Zurich.

Zuliani, M., Kenney, C. S., and Manjunath, B. S., 2005, The Multiransac Algorithm and its Application to Detect Planar Homographies, In: *Proc. IEEE International Conference on Image Processing*, Genova, Italy.